

Magnetic properties of $(\text{Nd}, \text{Sm})_5\text{Fe}_{17}$

This article has been downloaded from IOPscience. Please scroll down to see the full text article.

1997 J. Phys.: Condens. Matter 9 9353

(<http://iopscience.iop.org/0953-8984/9/43/019>)

View [the table of contents for this issue](#), or go to the [journal homepage](#) for more

Download details:

IP Address: 171.66.16.209

The article was downloaded on 14/05/2010 at 10:53

Please note that [terms and conditions apply](#).

Magnetic properties of $(\text{Nd}, \text{Sm})_5\text{Fe}_{17}$

Chin Lin, Cong-Xiao Liu, Yun-Xi Sun and Zun-Xiao Liu

Department of Physics, Peking University, Beijing, People's Republic of China

Received 1 June 1997, in final form 5 August 1997

Abstract. $(\text{Nd}_{1-x}\text{Sm}_x)_5\text{Fe}_{17}$ and $(\text{Nd}_{1-x}\text{Sm}_x)_5(\text{Fe}_{1-y}\text{Ti}_y)_{17}$ samples were prepared by arc melting and then annealed in vacuum. For the Nd-rich samples, $\text{Nd}_5\text{Fe}_{17}$ type structure was obtained by a long annealing (600 °C, 48 d); for the Sm-rich samples, it was obtained by a short annealing (750–900 °C, 1 d). With increasing Sm content, the easy magnetization direction converts from the basal plane to the *c*-axis. An easy-*c*-axis anisotropy is observed at room temperature for $x \geq 0.3$. A small amount of Ti favours the formation of $\text{Nd}_5\text{Fe}_{17}$ type structure only in the Sm-rich samples. It destroys this structure in the Nd-rich samples.

1. Introduction

$\text{Nd}_5\text{Fe}_{17}$ is a new stable ferromagnetic phase in the binary Nd–Fe system [1]. A revised phase diagram is reported [2]. Single-crystal x-ray diffraction [3] and powder sample neutron diffraction [4] analyses showed that its crystal structure belongs to the hexagonal space group $P6_3/mcm$ with 12 formula units per cell. Magnetic measurements [5, 6] and Mossbauer spectra [7] showed that the average moment per Fe atom $\mu_{Fe} = 2.12\mu_B$ and $\mu_{Nd} = 2.44\mu_B$ at 1.5 K. Unfortunately, $\text{Nd}_5\text{Fe}_{17}$, similar to $\text{Nd}_2\text{Fe}_{17}$, has an easy-plane anisotropy [6]. It is not considered to be a promising permanent magnetic material. To obtain easy-*c*-axis anisotropy, Nd has to be replaced by a rare earth element which has a different-sign Stevens factor α_J with that of Nd. Sm meets this demand. Actually, high-coercive-force Sm–Fe–Ti alloys have been produced by sputtering [8], mechanical alloying [9], melt-spinning [10], and conventional powder metallurgical method [11]. Careful investigation of the x-ray diffraction patterns of these Sm–Fe–Ti alloys [12] showed that they have $\text{Nd}_5\text{Fe}_{17}$ type structure. $\text{Sm}_5(\text{Fe}, \text{Ti})_{17}$ has a high coercive force but a low saturation magnetization due to the small moment of Sm. Furthermore, it seems necessary to add a small amount of Ti. To our knowledge, $\text{Sm}_5\text{Fe}_{17}$ has only been formed by sputtering film until now [13], and its coercive force is much lower than that of $\text{Sm}_5(\text{Fe}, \text{Ti})_{17}$ film. Our previous work [5] showed that $\text{Nd}_5\text{Fe}_{17}$ type structure is maintained when 10% Nd is substituted by Sm, Gd, and Y. All of them have an easy-plane anisotropy. Here we substitute Nd by Sm in the entire range of composition to study the crystallographic and magnetic properties. An easy-*c*-axis anisotropy is observed at room temperature when 30% Nd is substituted by Sm. Besides, a small amount of Ti is added in some samples to investigate its effect on the formation of the $\text{Nd}_5\text{Fe}_{17}$ type structure.

2. Experiment

$(\text{Nd}_{1-x}\text{Sm}_x)_5(\text{Fe}_{1-y}\text{Ti}_y)_{17}$ ($x = 0, 0.05, 0.10, 0.15, 0.2, 0.3, 0.5, 0.7, 0.9, 1.0$; $y = 0, 0.06, 0.09$) samples were prepared by arc melting (Nd, Sm) and Fe in the proportion of 1 to 3 under

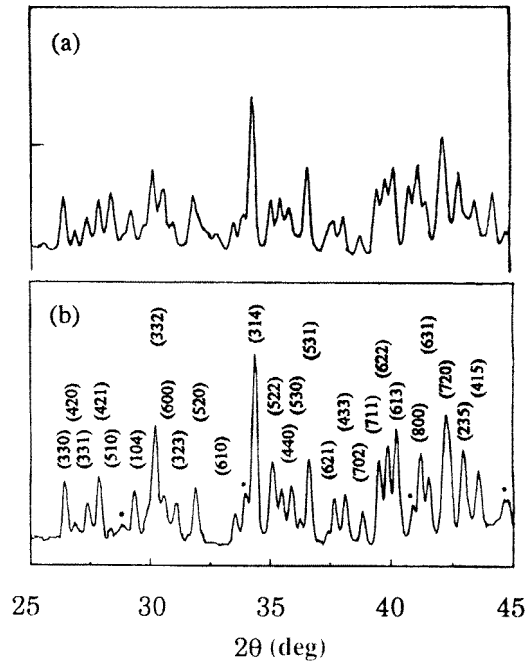


Figure 1. X-ray diffraction patterns. (a) $(\text{Nd}_{0.3}\text{Sm}_{0.7})_5(\text{Fe}_{0.94}\text{Ti}_{0.06})_{17}$, (b) $(\text{Nd}_{0.7}\text{Sm}_{0.3})_5\text{Fe}_{17}$.

Table 1. Lattice parameters and Curie temperature of the samples studied.

	X	a (Å)	c (Å)	T_c (K)
$(\text{Nd}_{1-x}\text{Sm}_x)_5\text{Fe}_{17}$	0.0	20.207	12.341	507
	0.05	20.218	12.375	511
	0.10	20.204	12.354	510
	0.15	20.212	12.350	515
	0.20	20.222	12.340	519
	0.30	20.196	12.360	527
	0.50	20.241	12.191	
$(\text{Nd}_{1-x}\text{Sm}_x)_5(\text{Fe}_{0.94}\text{Ti}_{0.06})_{17}$	0.50	19.913	12.435	557
	0.70	20.209	12.374	564
	0.80	20.182	12.330	570
$(\text{Nd}_{1-x}\text{Sm}_x)_5(\text{Fe}_{0.91}\text{Ti}_{0.09})_{17}$	1.00	20.183	12.348	598

a purified argon atmosphere. The samples were annealed in vacuum at different temperature for different time. Structural analyses were carried out on powder samples with a Rigaku D/Max-RB diffractometer using Cu $K\alpha$ radiation. Thermomagnetic curves were measured with a vibrating sample magnetometer at a low field. X-ray diffraction and thermomagnetic analyses showed that the Nd-rich ($x \leq 0.5$) samples, similar to $\text{Nd}_5\text{Fe}_{17}$ [1, 5], annealed at 600°C for 48 d have the $\text{Nd}_5\text{Fe}_{17}$ type structure. Small amounts of metallic Nd(Sm) and/or $(\text{Nd, Sm})_2\text{Fe}_{17}$ were found in some samples. When $x \geq 0.5$, samples annealed in the same conditions contain R_5Fe_{17} , R_2Fe_{17} and RFe_2 phases. The amount of R_5Fe_{17} phase

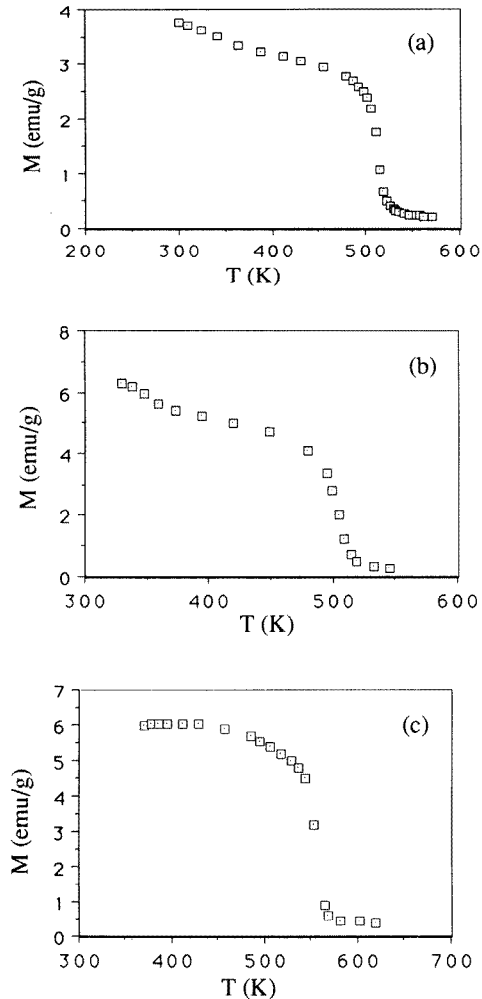


Figure 2. Thermomagnetic curves: (a) $(Nd_{0.7}Sm_{0.3})_5Fe_{17}$; (b) $(Nd_{0.5}Sm_{0.5})_5Fe_{17}$; (c) $(Nd_{0.3}Sm_{0.7})_5(Fe_{0.94}Ti_{0.06})_{17}$.

decreases with increasing Sm content. Sm-rich samples, similar to $Sm_5(Fe, Ti)_{17}$ [11], were annealed at higher temperature (750–900 °C) for 1 d. Experimental results showed that Ti addition favours the formation of Nd_5Fe_{17} type structure only in the Sm-rich samples. It destroys this structure in the Nd-rich samples. Samples having Nd_5Fe_{17} type structure are $(Nd_{1-x}Sm_x)_5Fe_{17}$ ($x \leq 0.5$) and $(Nd_{1-x}Sm_x)_5(Fe, Ti)_{17}$ ($x \geq 0.5$).

Magnetic measurements were performed at fields up to 70 kOe in the temperature range of 1.5 K to room temperature. Samples were pulverized. The particle sizes were about 30 μm , which were sufficiently small to regard them as single crystallites. Powders were mixed with epoxy resin and filled in a plastic tube of cylindrical shape. The tube was placed in an external field of 10 kOe with its cylindrical axis parallel to the field direction at room temperature. Magnetic moments are aligned by the field. If the sample has an easy magnetization direction (EMD) parallel to the c -axis, the c -axis of all single crystallites can be aligned parallel to the direction of magnetic field (cylindrical axis). If the sample has an

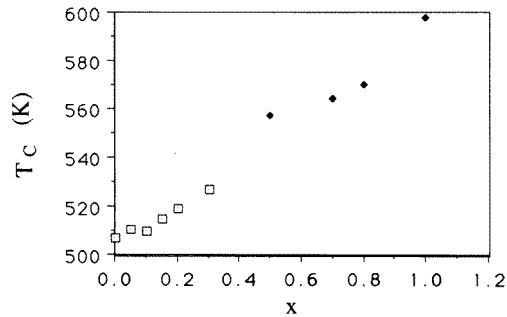


Figure 3. Composition dependence of the Curie temperature. □: $(\text{Nd}_{1-x}\text{Sm}_x)_5\text{Fe}_{17}$. ◆: $(\text{Nd}_{1-x}\text{Sm}_x)_5(\text{Fe}_{0.94}\text{Ti}_{0.06})_{17}$ and $\text{Sm}_5(\text{Fe}_{0.91}\text{Ti}_{0.09})_{17}$.

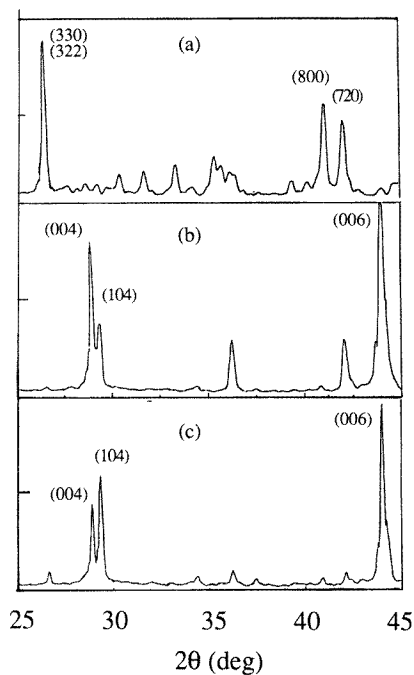


Figure 4. X-ray diffraction patterns of aligned powders: (a) $(\text{Nd}_{0.85}\text{Sm}_{0.15})_5\text{Fe}_{17}$; (b) $(\text{Nd}_{0.7}\text{Sm}_{0.3})_5\text{Fe}_{17}$; (c) $(\text{Nd}_{0.5}\text{Sm}_{0.5})_5(\text{Fe}_{0.94}\text{Ti}_{0.06})_{17}$.

easy-plane anisotropy, the basal plane can be aligned parallel to the cylindrical axis. X-ray diffraction analyses were performed on aligned samples with the surface perpendicular to the cylindrical axis. For the easy-*c*-axis samples, the $(00l)$ reflections will be enhanced remarkably. In the contrast, for the easy-plane samples, the $(hk0)$ reflections will be enhanced remarkably.

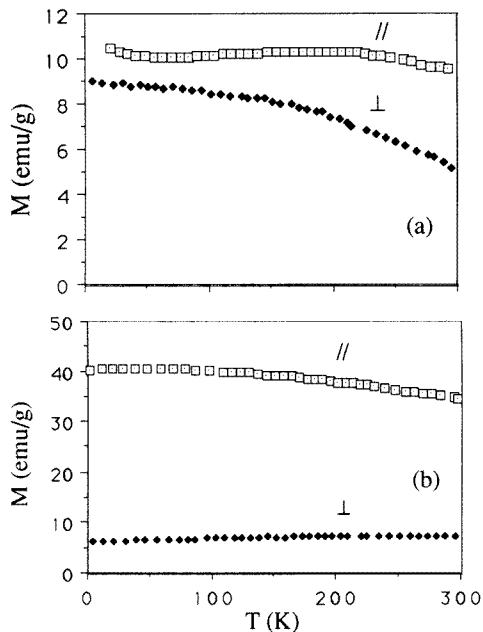


Figure 5. Temperature dependence of the magnetization parallel (\parallel) and perpendicular (\perp) to the alignment direction (\parallel c -axis or \perp c -axis) in a field of 2 kOe: (a) $(Nd_{0.7}Sm_{0.3})_5Fe_{17}$; (b) $(Nd_{0.5}Sm_{0.5})_5(Fe_{0.94}Ti_{0.06})_{17}$.

3. Results and discussion

X-ray diffraction patterns of $(Nd_{0.3}Sm_{0.7})_5(Fe_{0.94}Ti_{0.06})_{17}$ and $(Nd_{0.7}Sm_{0.3})_5Fe_{17}$ are shown in figure 1(a) and (b), respectively. These patterns are rather line rich, and can be indexed on the basis of Nd_5Fe_{17} type structure. Impurity phases are marked by small dots. Figure 2(a)–(c) is the thermomagnetic curves of $(Nd_{0.7}Sm_{0.3})_5Fe_{17}$, $(Nd_{0.5}Sm_{0.5})_5Fe_{17}$ and $(Nd_{0.3}Sm_{0.7})_5(Fe_{0.94}Ti_{0.06})_{17}$, respectively. The small kink at about 370 K in figure 2(b) indicates the presence of a small amount of R_2Fe_{17} phase. The Curie temperature is determined by plotting M^2 against T near T_c and extrapolating the linear part to $M = 0$. The composition dependence of T_c is shown in figure 3. Lattice parameters and Curie temperatures are listed in table 1.

Nd_5Fe_{17} has an easy-basal-plane anisotropy, but Sm_5Fe_{17} has an easy- c -axis anisotropy. Therefore, a transition from easy plane to easy axis must occur in quasi-binary region when x increases from 0 to 1. The x-ray diffraction patterns of aligned powders for $(Nd_{0.85}Sm_{0.15})_5Fe_{17}$, $(Nd_{0.7}Sm_{0.3})_5Fe_{17}$, and $(Nd_{0.5}Sm_{0.5})_5(Fe_{0.94}Ti_{0.06})_{17}$ are shown in figure 4(a)–(c), respectively. The intensities of (330), (800), and (720) reflections are the strongest in (a); but (006), (004), and (104) reflections are the strongest in (b) and (c), indicating that the easy magnetization direction converts from the basal plane to the c -axis at room temperature when x increases from 0.15 to 0.3. The alignment of the $x = 0.5$ sample is better than that of the $x = 0.3$ sample. The temperature dependences of magnetization parallel (M_{\parallel}) and perpendicular (M_{\perp}) to the alignment direction for $(Nd_{0.7}Sm_{0.3})_5Fe_{17}$ and $(Nd_{0.5}Sm_{0.5})_5(Fe_{0.94}Ti_{0.06})_{17}$ are shown in figure 5(a) and (b), respectively. With decreasing temperature down to 1.5 K, M_{\parallel} and M_{\perp} vary smoothly, indicating no spin reorientation occurs. To further investigate anisotropy, magnetization curves of aligned $(Nd_{0.7}Sm_{0.3})_5Fe_{17}$

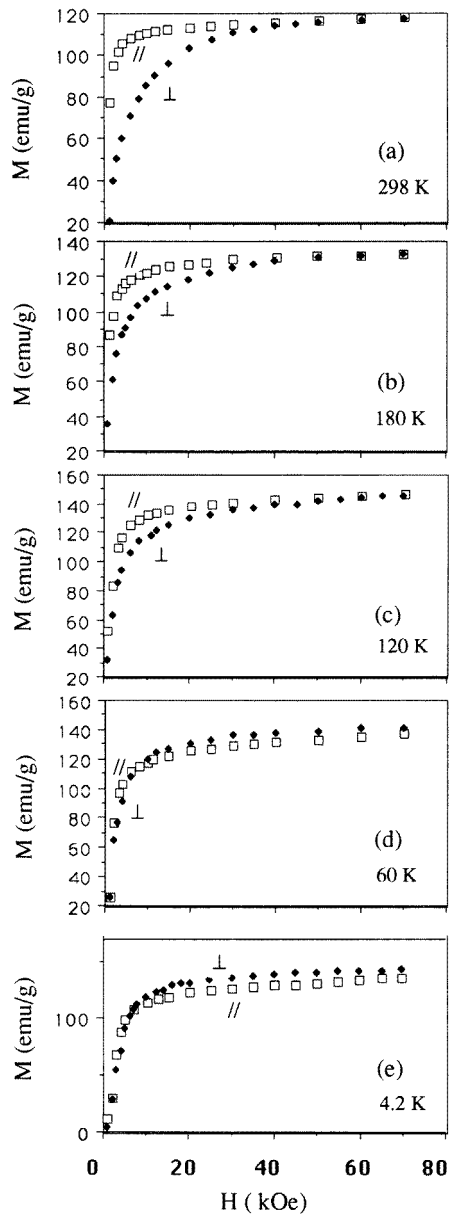


Figure 6. Magnetization curves parallel (\parallel) and perpendicular (\perp) to the alignment direction (\parallel c -axis or \perp c -axis) for $(\text{Nd}_{0.7}\text{Sm}_{0.3})_5\text{Fe}_{17}$ at different temperatures: (a) $T = 298$ K; (b) $T = 180$ K; (c) $T = 120$ K; (d) $T = 60$ K; (e) $T = 4.2$ K.

at different temperatures are measured and are shown in figure 6. It is clear that the difference between M_{\parallel} and M_{\perp} decreases with decreasing temperature, indicating a decreasing anisotropy. When $T \leq 60$ K, this sample is almost isotropic and M_{\parallel} is almost the same as M_{\perp} . The Stevens factor α_J is of different sign for Nd and Sm. They have different anisotropy. When Nd is substituted by Sm, the resultant anisotropy is determined

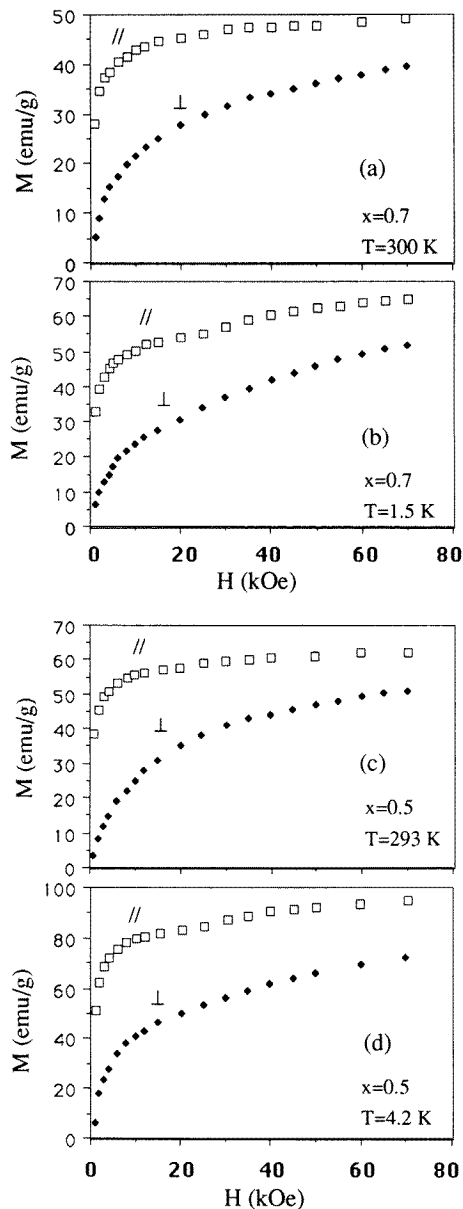


Figure 7. Magnetization curves parallel (\parallel) and perpendicular (\perp) to the alignment direction (\parallel c -axis or \perp c -axis) at different temperatures for $(Nd_{1-x}Sm_x)_5(Fe_{0.94}Ti_{0.06})_{17}$: (a) $x = 0.7$, $T = 300$ K; (b) $x = 0.7$, $T = 1.5$ K; (c) $x = 0.5$, $T = 293$ K; (d) $x = 0.5$, $T = 4.2$ K.

by the competition between anisotropies of Nd and Sm. For $x = 0.3$, the contribution of Sm to the anisotropy is almost the same as that of Nd at low temperature. The resultant anisotropy is very small. With increasing temperature, the anisotropy of Nd decreases more quickly than that of Sm. The anisotropy of Sm is dominant at room temperature, as shown by the x-ray diffraction pattern of aligned powders in figure 4(b). When $x \geq 0.5$,

the anisotropy of Sm is dominant even at low temperature. Figure 7(a)–(d) shows the magnetization curves of $(\text{Nd}_{0.3}\text{Sm}_{0.7})_5(\text{Fe}_{0.94}\text{Ti}_{0.06})_{17}$ and $(\text{Nd}_{0.5}\text{Sm}_{0.5})_5(\text{Fe}_{0.94}\text{Ti}_{0.06})_{17}$ at room temperature and low temperature, respectively. The anisotropy field was deduced from the extrapolated intersection of M_{\parallel} and M_{\perp} curves. $H_A = 170$ kOe at 1.5 K for $(\text{Nd}_{0.3}\text{Sm}_{0.7})_5(\text{Fe}_{0.94}\text{Ti}_{0.06})_{17}$.

In conclusion, $\text{Nd}_5\text{Fe}_{17}$ type structure can be formed in the entire range of composition. The competition between anisotropy of Nd and Sm results in a conversion in the easy magnetization direction from the basal plane to the c -axis when Sm content increases. An easy- c -axis anisotropy is observed at room temperature when $x \geq 0.3$. The effect of Ti addition on the formation of $\text{Nd}_5\text{Fe}_{17}$ type structure in Nd-rich samples is opposite to that in Sm-rich samples. It is favourable only for the Sm-rich samples.

Acknowledgments

Project 19374001 was supported by the National Science Foundation of China. We are grateful to Professor Shun-Ying Chen for x-ray diffraction experiments.

References

- [1] Schneider G, Landgraf F J G, Villas-Boas V, Bezerra G H, Missell F P and Ray A E 1989 *Mater. Lett.* **8** 472
- [2] Landgraf F J G, Schneider G, Villas-Boas V and Missell F P 1990 *J. Less-Common Met.* **163** 209
- [3] Moreau J M, Paccard L, Nozieres J P, Missell F P, Schneider G and Villas-Boas V 1990 *J. Less-Common Met.* **163** 245
- [4] Chin Lin, Cong-Xiao Liu, Yun-Xi Sun, Zun-Xiao Liu, Dong-Feng Chen, Cheng Gou, Kai Sun and Ji-Lian Yang *J. Magn. Magn. Mater.* submitted
- [5] Cong-Xiao Liu, Yun-Xi Sun, Zun-Xiao Liu and Chin Lin 1994 *J. Appl. Phys.* **76** 6766
- [6] Landgraf F J G, Missell F P, Rechenberg H R, Schneider G, Villas-Boas V, Moreau J M, Paccard L and Nozieres J P 1991 *J. Appl. Phys.* **70** 6125
- [7] Nozieres J P and Rechenberg H R 1991 *Solid State Commun.* **79** 21
- [8] Kamprath N, Qian X R, Hegde H and Cadieu F J 1990 *J. Appl. Phys.* **67** 4948
- [9] Schnitzke K, Schultz L, Wecker J and Katter M 1990 *Appl. Phys. Lett.* **56** 587
- [10] Katter M, Wecker J and Schultz L 1990 *Appl. Phys. Lett.* **56** 1377
- [11] Huang M Q, Simizu S, Miller K and Wallace W E 1993 *J. Appl. Phys.* **73** 5902
- [12] Stadelmaier H H, Schneider G, Henig E-Th and Ellner M 1991 *Mater. Lett.* **10** 303
- [13] Cadieu F J, Hegde H, Rani R, Navarathna A and Chen K 1991 *Mater. Lett.* **11** 284